ASIA TURBOMACHINERY & PUMP SYMPOSIUM
23-26 FEBRUARY 2021
SHORT COURSES: 22 FEBRUARY 2021

PERFORMANCE TEST OF FULL-SIZE WET TOLERANT COMPRESSOR

Alberto Milani
Senior Systems Engineer
Baker Hughes
Florence, IT

Luca Scarbolo
Business Operations Specialist
Baker Hughes
Florence, IT

Manuele Bigi
Senior Engineer
Baker Hughes
Florence, IT

Emanuele Rizzo
Senior Engineer
Baker Hughes
Florence, IT

Silvia Evangelisti
Lead Engineer Testing
Baker Hughes
Florence, IT

Maria Vittoria Borghesi
Lead Engineer Testing
Baker Hughes
Florence, IT

Giuseppe Vannini
Principal Rotordynamics Engineer
Baker Hughes
Florence, IT

Giuseppe Sassanelli
Senior Engineering Manager
Baker Hughes
Florence, IT

ABSTRACT

Standard centrifugal compressors (CC) are designed to process dry gas or gas mixed with negligible amount of liquid. Significant liquid content, namely liquid mass fraction (LMF) up to 30%, yield to rapid mechanical deterioration of the CC internals. Field experiences have shown significant erosion and corrosion of the compressor internals coupled with intense fouling. Furthermore, even a small liquid ingestion is associated with non-negligible CC performance variations; as machine head and efficiency are both affected together with the machine rotordynamics. However, the compression of gas containing significant amounts of liquid phase can yield to some substantial advantages in size and efficiency as liquid removal stations can be reduced (and eventually eliminated). Thus, the compression station footprint and cost can be reduced accordingly with relevant impact on the layout and cost of subsea stations. Moreover, the introduction of selected wet tolerant features can yield to increased reliability of machines where wet conditions (or mild wet conditions) are triggered during off-design operations.

With the aim of providing a reliable technology for wet gas applications the OEM has developed a full size wet tolerant compressor prototype in which the machine lay-out, material selection, rotordynamics and aerodynamics were specifically designed to process significant liquid mass fractions (i.e. up to 30%).

The wet tolerant prototype was tested in a closed loop where rich gas is laden with condensate hydrocarbons and water. The compressor driven by a 2.8MW electric VFD motor reaches operating speeds ranging from 8807rpm to 13210rpm. A test matrix was designed to explore a wide range of inlet pressures (20bar -110bar) with liquid contents spanning from 5% to 30% of the total mass flow rate. The compressor performance was measured either with ASME-PTC10 standards (flange-to-flange) and internal dedicated instrumentation. Moreover, the whole test rig was instrumented and monitored. Internal fouling and erosion were investigated with borescope inspections within the test campaign and with bundle removal after the test campaign.

INTRODUCTION

Standard centrifugal compressors (CC) are conceived and designed to process dry gases, namely gases with no (or negligible) liquid content. Due to both application and operations, a compressor can seldom operate gas laden with liquid content. Typical applications are upstream compressor units in which liquid is a result of an incomplete gas-liquid separation, or process compressors in which a certain amount of liquid is injected for cooling and washing purposes.

The most common solution to avoid liquid ingestion, relies on the installation of upstream separation devices. Although necessary, these separation stations do significantly increase the footprint, the installation complexity, and the operating costs of the compression stations.

One viable way to overcome or reduce size and costs associated with the plant equipment is the use of Wet Gas Compression (WGC), namely the compression of a gas containing a significant amount of liquid. Through this technology the upstream gas-liquid separators can be reduced in size (or even removed), thus reducing the installation and operating cost of the overall compression stations. The advantages of the WGC technology have been assessed by several authors in recent years (Brenne et al., Bertoneri et al and Fabbrizzi et al). They also highlight the applicability to subsea installations in which WGC technology has shown promising capabilities in the reduction of compression stations footprint. Moreover, experimental validations of CC operating in wet conditions have shown that a WGC does not limit the operating range of the CC (Grüner et al., Minghong et al.).

To benefit from a WGC application, CC design should be tailored to cope with the presence of liquid. Material selection, a dedicated mechanical and aerodynamic design are required to limit erosion and corrosion of the internals, and to ensure API compliant vibration levels as well as performance prediction and machine operability.

In recent years an OEM has investigated all the aspects of WGC CC design. Dedicated experimental campaigns on material characteristics, rotordynamics, mechanical architecture and aerodynamics have been carried out under wet conditions. Based on the results of the test campaigns the OEM has defined a design approach, that substantially increases the liquid tolerance of the CC.
Based on this design approach, a full-size WGC CC was designed and tested under real upstream process conditions for around 2800 hours before bundle inspection. Among those only about a 1000hrs were part of the WGC test (850hrs in wet plus 150hrs to test the dry curves). The rest were accumulated by the WGC but not part of the test itself. This paper describes the test rig, and test campaign providing the assessment of compressor performance, operability and rotordynamics. Finally, a complete post-test bundle inspection is presented.

WET GAS COMPRESSOR DESIGN

The wet gas pilot is a two stages centrifugal compressor designed to treat process gas with a liquid presence up to 30% LMF under continuous operation. The liquid can be both hydrocarbon condensate and/or water. Special materials and coatings have been used for this application to better withstand liquid droplet erosion (LDE), as well as contaminants presence in the gas such as chlorides and carbon dioxide.
The rotor is supported by two journal bearings, both drive end (DE) and non-drive end (NDE) have tilting pads. The thrust bearing is equipped with 8 load cells on the pads, four on the active side pads, and four on the inactive side pads. The compressor has been equipped with tandem dry gas seals (DGS). Each seal, DE and NDE, is composed of a barrier seal (CSE carbon ring type), a secondary seal (atmospheric side), and a primary seal (process side). Primary DGS is buffered with process gas treated, filtered, and heated by Seal Gas Conditioning Skid (SGCS), while secondary DGS is buffered with nitrogen, treated by Seal Gas Panel (SGP).

The compressor is equipped with both standard instrumentation (radial and axial vibration sensors and journal and thrust bearing temperature probes) and dedicated special instrumentation:
• static and dynamic pressure probes at several flow path sections to monitor static pressure trends and identify static and dynamic compressor behavior
• resistance temperature detector (RTD) and pressure transmitter (PT) static probes at compressor interstage location, to provide interstage measurement
• level transmitters (LT) probes at several compressor chambers to verify liquid level inside machine
• RTDs and flow measurement on lube oil system to evaluate mechanical losses

• torquemeter on high speed coupling to measure the compressor mechanical absorbed power.

Distinctive design features are adopted to manage heavy liquid presence. The inlet plenum and Inlet Guide Vane (IGV) diaphragm have been properly coated to avoid erosion. The first impeller has been designed to promote an early breakup of droplets, ensuring a well atomized liquid flow over the entire flow path. The tailored design of impeller blades promotes droplet break up by increasing the inertial effects responsible for the droplet breakup. The erosion of typical impeller affected areas is minimized by smoothing the flow path curvature. The design of the first impeller is thus a compromise between the erosion requirements and the aerodynamic performance. A dedicated validation test of the wet tolerant impeller design was performed to compare with a standard impeller, aerodynamic performance, and erosion resistance capability (Falomi et al. 2016). The impellers are manufactured in Inconel, while diaphragms are manufactured with martensitic stainless steel and coated where possible. In some parts of the compressor, due to constrains related to the introduction of the special probes, was not possible to coat. Discharge scroll is featured with extraction holes with different purposes. A first row of holes is used as the DGS auto-buffer source through the SGCS. Another row of holes allows the feeding of the balance drum shunt holes.

The momentum component of the thrust load under wet conditions might be subject to large variations due to the change of operating point as well as of the LMF. To manage these, the flow path of the machine is optimized adjusting the impeller foot seal diameters to smooth the thrust load gradient.

Rotordynamic design

The WGC rotordynamic design was inspired by encouraging results achieved during the qualification conducted by the OEM in previous years. Worth of mention is the successful test on a single stage prototype, whose results were published in Vannini, Bertoneri et al. (2014). From now on this reference machine will be addressed as the WGC prototype.

The special devices applied to the WGC to manage the liquid content are: Pocket Damper Seal (PDS); Special Shunt holes and "Open" Swirl brakes and Tooth On Rotor (TOR) laby seals. Journal bearings are of tilting pad type, a common OEM design.

Pocket Damper Seal

The design of the compressor foreseen the use of a PDS. This seal demonstrated to suppress a severe liquid induced whirl in the previous test performed by OEM, see Vannini, Bertoneri. This final design was even validated through a multiphase flow CFD analysis which confirmed the PDS ability to stop the liquid whirl inside the pockets and it also provided the dynamic coefficients for the rotodynamic stability check under wet conditions. Figure 1 shows an almost zero expected liquid content into the seal when the compressor inlet LVF is 3% (around 30%LMF).

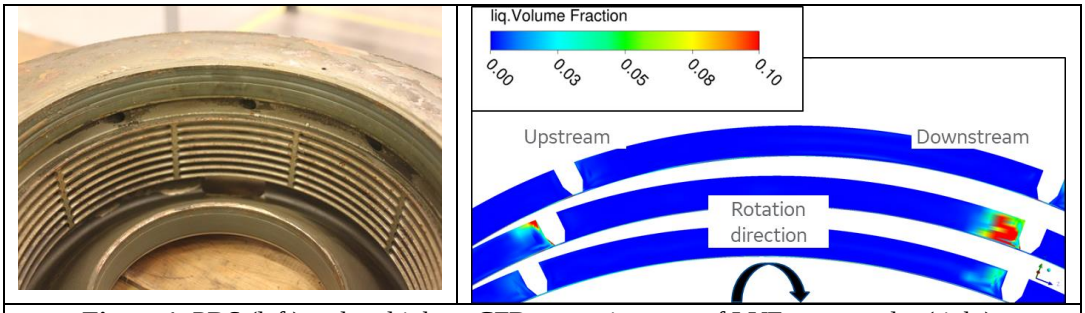

Figure 1: PDS (left) and multiphase CFD output in terms of LVF contour plot (right).

To the Authors' opinion the PDS force coefficients (even under dry conditions) are subject to more uncertainty with respect to other most common damper seals coefficients (e.g. honeycomb or hole pattern seals) since they are not widely adopted by OEMs and the dedicated technical research is less extensive. The relevant predictions at design phase were based on a bulk flow code developed by Texas A&M Turbomachinery Laboratory, which was considered as the best available tool, refer to Li, San Andres.

Furthermore, a set of calibration factors coming from an internal OEM test campaign, see Vannini, Cioncolini et al., was applied to get a tuned bulk flow version.

Table 1 shows the different predictions in terms of both frequency and log dec for the rotor first forward mode (the most relevant one for the stability check). It is interesting to notice the trend of log dec increasing more and more moving from the original coefficients predicted by the simple bulk flow code up to the coefficients predicted by CFD. The final field stability scenario was even better than the CFD prediction and it is shown in Figure 13.

Bulk flow code		Tuned bulk flow code		CFD	
FN1 [cpm]	Log Dec [-]	FN1 [cpm]	Log Dec [-]	FN1 [cpm]	Log Dec [-]
6503	0.48	6755	0.57	7183	0.89

Table 1: Summary of stability analysis (first natural frequency and Log Dec) with PDS in dry operation

Special Shunt holes

As it is well known from the technical literature, shunt holes are a powerful device to increase the rotordynamic stability through the control of gas swirl at a seal entrance. For this wet gas application, the design was optimized to route away any liquid content into the seal. For this reason, a specific patent was filed, see Bertoneri, Vannini.

Open swirl brakes and TOR seals

Tooth On Rotor (TOR) geometry was selected for the impeller eye seals because of their better capability to evacuate liquid. Due to the centrifugal force acting on rotating teeth, liquid is streamed to the main leakage path and expelled through the gas leakage flow. This schematic process was demonstrated by previous CFD work, see Vannini, Bertoneri, Nielsen.

Swirl brakes were adopted to ensure a very low swirl at the seal entrance. Since this was the first time to apply such device in wet conditions, a multiphase CFD analysis was conducted to verify swirl brakes efficacy. The design adopted here has been a so called "open design" to avoid liquid flooding while reducing the swirl. As shown on Figure 2, the liquid level is expected to be low enough in between the vanes with some minor fill-up in the top region far away by the rotor.

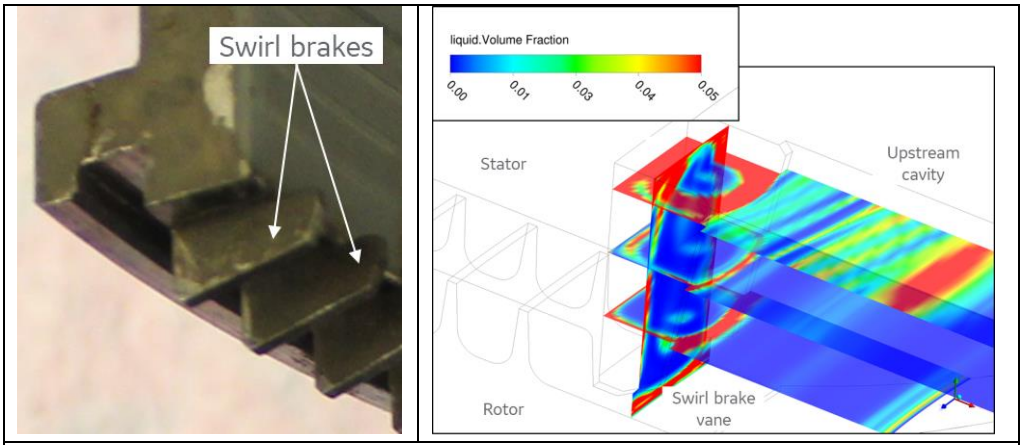

Figure 2: "Open design" swirl brakes (left), and multiphase CFD in terms of LVF (right).

The aerodynamic performance of this kind of swirl brakes (e.g. the gas swirl level downstream of the vanes) is expected to be very similar for both dry and wet conditions.

TEST RIG

The K-lab test facility is located at Kårstø processing plant on the west coast of Norway. The K-lab has two separate wet gas test loops both capable of full-scale testing with real hydrocarbon conditions (realistic composition, pressure, temperature, gas/liquid flowrate and power). Figure 3 shows the process flow diagram of the test loop.

Gas flowing over the top of the Gas/Liquid separator passes a suction filter before the gas flow is measured in a flow orifice. Downstream the flow orifice an ASME PTC 10 pressure and temperature measurement section is installed. Next the gas flows through a liquid injection mixer before it again flows through a PTC 10 pressure and temperature section located on compressor suction (here the pure gas or liquid/gas mixture will be measured). On the compressor discharge the fluid flows through a PTC 10 temperature and pressure section before it passes the coolers targeting the compressor suction temperature set point. The gas or gas/liquid mixture is finally returned to the gas/liquid separator.

The liquid flowing through the bottom of the gas/liquid separator flows through a liquid pump and further into a liquid/liquid separator where the condensate and water are separated. The water phase is further led through a second Liquid/Liquid separator ensuring complete separation of condensate from the water phase. Two separate metering stations have been used for condensate and water; each liquid metering station is composed by three Coriolis meters of different size allowing high liquid measurement accuracy for a

wide range of flow rates. The water and condensate are further led through the liquid heater and/or liquid cooler, targeting the compressor suction temperature set point, and finally led to the liquid mixer located close to compressor suction.

Thermodynamic mixture model

An online thermodynamic mixture model calculates the physical properties, compositions, and flow rates of individual phases (total bulk fluid, condensate phase, water phase and gas phase) at designated locations throughout the test loop. These points are called flash points and are locations with known pressure, temperature, and mass/molar flowrates. The model is based on total loaded (filled) amounts of water, condensate, and gas all with known composition, in addition to the known total volumes of the loop. Consequently, this system allows for a continuously monitoring of properties and performance evaluation of the test object.

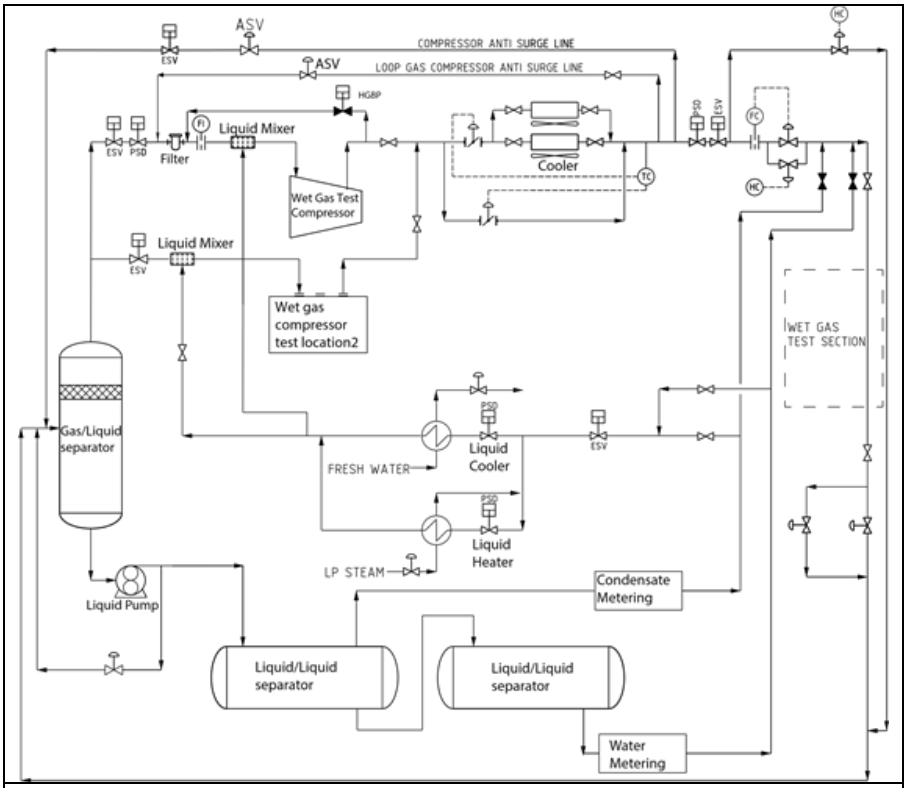

Figure 3: Process Flow diagram K-Lab multiphase loop

TEST MATRIX AND TEST EXECUTION

The test matrix covered the following test parameters range:

- Speed: 8807÷13210rpm
- Suction pressure: 20÷110bara
- LMF: 0÷30%
- Liquid type: HC condensate, water, HC condensate + water

The test was composed of these steps:

- Performance tests: each performance curve of the Test Matrix was explored from overflow to part-flow (5 test points) in compliance with ASME PTC10

- Fixed discharge pressure tests: to replicate a common site conditions where the delivered pressure is the constraint for the machine operation independently from LMF. Targeted discharge pressure was reached by adjusting the rotating speed at each different LMF

- Surge test: to verify any modification of the surge line at various LMF. In addition, anti-surge controller, tuned for dry condition, was tested to verify his behavior accuracy under wet conditions too

- Wet shutdown, slug test, wet startup from flooded conditions: to demonstrate compressor operability during transient

conditions at different LMF and compressor capability to withstand upset process conditions

- 72hrs accelerated erosion test: compressor running at MCS and 30% LMF continuously for 72hrs.
- Fouling test: to assess fouling effects on compressor performance and verify the effectiveness of online washing cycles

Compressor run for 850hrs in wet conditions during WGC test.

PERFORMANCE TEST AND PERFORMANCE PREDICTION

Thermodynamic Performance Calculations

The performance calculation of a WGC requires a tailored approach due to the non-negligible liquid content. The thermodynamic framework here adopted is based on the works of Falomi et al.. Some extensions and generalizations are introduced to consider the change in composition due to different condensation/evaporation dynamics between the condensate components.

Liquid and gas properties have been computed considering the total injected mass flow, the overall components list and their molar fraction through a Peng-Robinson equation of state (EOS); the following equations for the mixture density, density ratio (DR) LMF and total inlet flow coefficient are used:

$$\frac{1}{\rho_l} = \frac{1}{\rho_{l,HC}} * \frac{\dot{m}_{l,HC}}{\dot{m}_{l,HC} + \dot{m}_{l,H_2O}} + \frac{1}{\rho_{l,H_2O}} * \frac{\dot{m}_{l,H_2O}}{\dot{m}_{l,HC} + \dot{m}_{l,H_2O}} \qquad DR = \frac{\rho_l}{\rho_g} \tag{1}$$

$$\phi = \frac{4 \cdot (Q_{1,g} + Q_{1,HC} + Q_{1,H_2O})}{\pi \cdot D_2^2 u_2}, \qquad LMF = \frac{m_{l,HC} + m_{l,H_2O}}{m_{l,HC} + m_{l,H_2O} + m_g} = \frac{m_{l,HC} + m_{l,H_2O}}{m_{tot}} \tag{2}$$

Where the liquid density (ρ_l) is the mass average density of the mixture composed by the hydrocarbons components (density ρ_{HC} and mass flow $m_{l,HC}$) and the water (density ρ_{H2O} and mass flow $m_{l,H2O}$). Based on the liquid density mixture and the dry gas density (ρ_g), the liquid to gas DR is defined in eq. (1).

The definition of inlet flow coefficient is extended considering the overall injected volume flow composed by the gas volume flow ($Q_{1,g}$), the liquid hydrocarbons ($Q_{1,HC}$) and liquid water ($Q_{1,H20}$). The liquid mass fraction of eq. (2) is defined as the overall injected liquid mass flow composed by hydrocarbons ($m_{1,HC}$) and water ($m_{1,H2O}$) mixture, divided by the overall ingested mass flow (m_{tot}), where also the gas mass flow (m_g) is included.

Due to the uncertainties in measuring the temperature under wet conditions (i.e. liquid film deposition on the probes, local heat transfer), the performance of the compressor is evaluated by pressure and mechanical measurements. The work coefficient (τ), namely the mass flow specific power normalized by the impeller peripheral speed, is defined through eq. (3):

$$\tau = \frac{H}{u_2^2} = \frac{P_{mech}}{m_{tot}\, u_2^2} \tag{3}$$

The total enthalpy jump (H) is computed considering the absorbed mechanical power (P_{mec}) and the total injected mass flow (m_{tot}). Since the two impellers have the same diameter, the choice of peripheral speed (u_2) is, in this case, trivial. To represent the actual gas power, the mechanical power is corrected to account for the mechanical losses of the journal and thrust bearings. The power absorbed by the bearings is computed through the lubricant enthalpy jump. The pressure ratio (PR), namely the ratio between the discharge pressure (p_2) and the suction pressure (p_1), is based on ASME-PTC10 since its accuracy is weakly affected by the presence of liquid.

The calculation of the polytropic transformation representative of a WGC requires care both from the theoretical and the measurement quality point of view. From a theoretical point of view, some general considerations must be made. Polytropic head definition is well-established in dry conditions and represent the gas transformation between two thermodynamic states with constant polytropic efficiency ($dH_p = vdp/\eta_p$). Due to the presence of two different phases, this assumption must be revised. The most straightforward approach is to use a two-fluid approach in which an ideal compressor-pump parallel elaborate separately the gas fraction (*1-LMF*) and the liquid fraction (*LMF*) delivering the same pressure and temperature. Although viable, this approach is not unique (i.e. mixture-based models) and, depending on the physical assumptions, the resulting polytropic head (H_p) and polytropic efficiency (η_p) will have slightly different values and different physical meanings. From the measurement quality, the uncertainties on the temperature calculation through a WGC will require to use a mechanical based calculation of the total enthalpy necessary for the polytropic head

calculation.
As a result, although viable, each approach towards the polytropic calculation in a WGC will have a different meaning from the dry calculation, making the values not directly comparable. Since the comparison between dry and wet polytropic transformations might be misleading, the results are not discussed in this paper, focusing on quantities directly connected to the compressor operation (PR, power). However, the thermodynamic modelling is still ongoing, since it is still important to identify a reference transformation to compare the compression efficiency modification in wet conditions.

All performances are normalized by the design flow coefficient (ϕ_n), the design suction pressure (p_n) and the rated speed (100%).

The performance curves are described through five test points: a central point close to the design flow coefficient (ϕ_n) and two points towards part-flow and overflow, respectively. While a dedicated session will take care of the surge limit.

Performance curves at fixed suction pressure:
Compressor performance in wet conditions is subjected to modifications that depend on the quantity of liquid injected and on the characteristics of the liquid. An example of the performance modifications as function of the LMF is reported in Figure 4 for the rated speed (100%) and design inlet pressure p_1/p_n=1. The results show a characteristic shift and tilting of the PR curves. In this case, when increasing the LMF, a higher PR and curve slope is observed towards part-flows region while a reduction of PR occurs in the overflow region. Due to the combination of curve tilt and shift, an intersection point between dry curves and wet curves can be observed. The shift and tilt of the curves is observed in all test campaign. Figure 4, 5 and 6 demonstrates that this intersection point moves in different position with regards to operating condition. More in details the two effects can be summarized as follows: a curve shift depends on the increased mixture density; a curve tilt depends on the balancing of intercooling effects (that dominate at part-flow) and increased multiphase losses (that dominate at overflow). The test points in the part-flow do stop in regions where no signals of surge (increments of vibrations or PR flattening) are observed while, by contrast, the overflow points are determined by the increased losses due to the wet operation of the test rig.

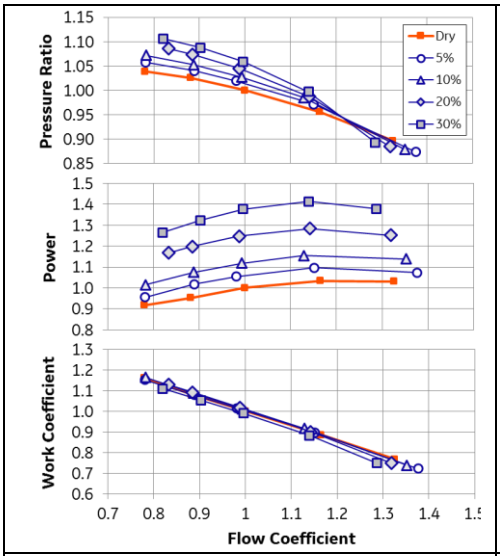

Figure 4: Compressor performance in dry and wet conditions at different LMF (5%÷ 30%) for p_1/p_n=1 and rated speed (100%).

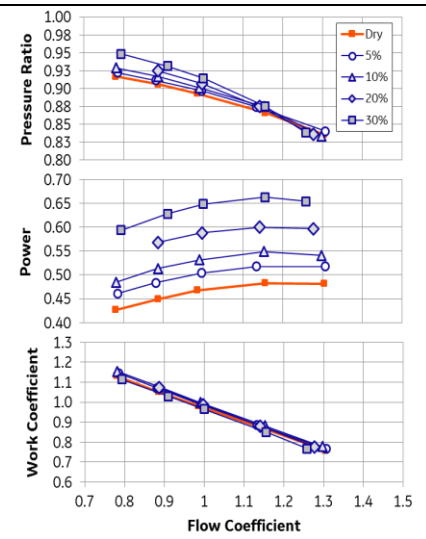

Figure 5: Compressor performance in dry and wet conditions at different LMF (5% ÷30%) for p_1/p_n=1 and minimum speed (78%).

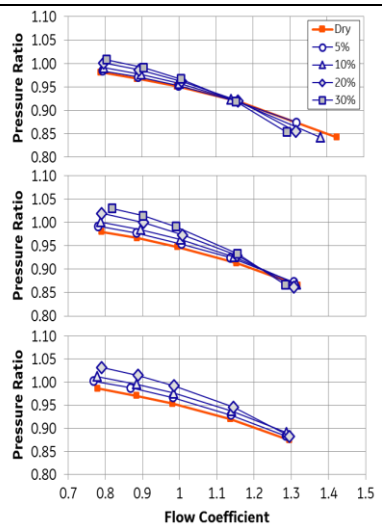

Figure 6: Effect of inlet pressure at 90% speed: normalized PR with inlet pressure p_1/p_n 0.54 (top), 1 (center), 1.25 (bottom).

The overall compression power increases with LMF with negligible modifications of the curves shape (Figure 4 and 5). This increment is largely due to the increased compressor mass flow for a given flow coefficient. The power variation due to the multiphase compression has a secondary role as shown by the normalized work coefficient. For a given flow coefficient the variation of the work coefficient is bounded to less than 5%. The behavior is repeated through all the other tested conditions, demonstrating that, for small density ratios (10 - 30), the largest component in the wet power increments are due to the increased mass flow. By contrast, the very high DR tests reported by Falomi et al. (atmospheric air-water test, DR > 800), have shown increments of compression power together with increments of the work coefficient, indicating significant power increments due to internal multiphase losses. A summary of the performance test execution and results is reported in Table 2.

Fixed	Variable	Summary of Results
Suction Pressure	LMF	shift and tilt of PR curve
		PR increment at part-flow (intercooling)
		PR reduction at overflow (enahced losses)
		Power increment mainly due to incremented mass flow (gas+liquid)
	Speed	LMF effects increase with speed (increased mass flow)

Table 2: Summary of performance test at fixed suction pressure.

Performance curves at fixed speed and variable suction pressure:
Figure 6 shows the effect of inlet pressure on the compressor PR for a DR range 10-30. The increment in inlet pressure results on a higher shift of the PR curves. At design flow coefficient (ϕ=1) the PR for LMF=20% increases roughly from 1.02 to 1.04 and 1.05 increasing the inlet pressure levels. The effects on curves tilt are limited, thus the intersection point with dry curve moves towards the overflow region. At the highest-pressure level, the CC operated in wet conditions delivers a PR always higher than in dry conditions. A summary of the performance test execution at fixed speed and variable suction pressure and results is reported in Table 3.

Fixed	Variable	Summary of Results
Speed	LMF	shift and tilt of PR curve
		PR increment at part-flow (intercooling)
		PR reduction at overflow (enahced losses)
		Power increment mainly due to incremented mass flow (gas+liquid)
	Suction Pressure	LMF effects are increased increasing suction pressure

Table 3: Summary of performance test at fixed speed

Compressor operation in wet conditions:
The effects of the CC maps modification, between dry and wet condition, are showed considering two different operating points, one at part-flow (point PR_1, PW_1, Figure 7) and one at overflow (point PR_2, PW_2, Figure 7).
In part-flow conditions, for a given normalized flow coefficient (i.e. ϕ = 0.85), the pressure ratio PR_1 is achieved in dry conditions at the rated speed (100%) while, thanks to the curves shift, it is delivered with a lower speed (90%) in wet conditions (LMF = 30%). Thanks to the reduced speed in wet conditions, the compression power remains essentially the same, confirming the fact that most of the increased power is related to the increased mass flow.

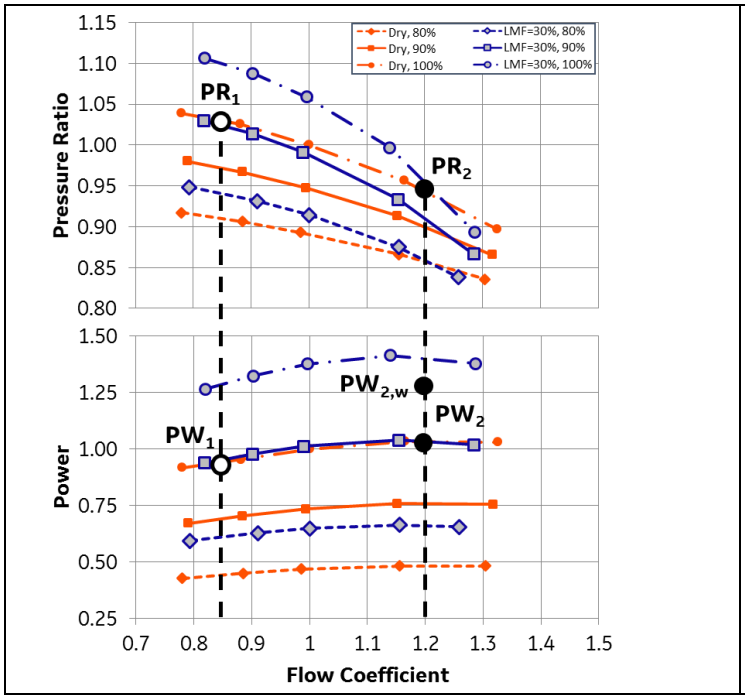

Figure 7: Compressor map (80%-90%-100% speed) in dry and wet conditions (LMF = 30%) for design inlet pressure p_1/p_n=1

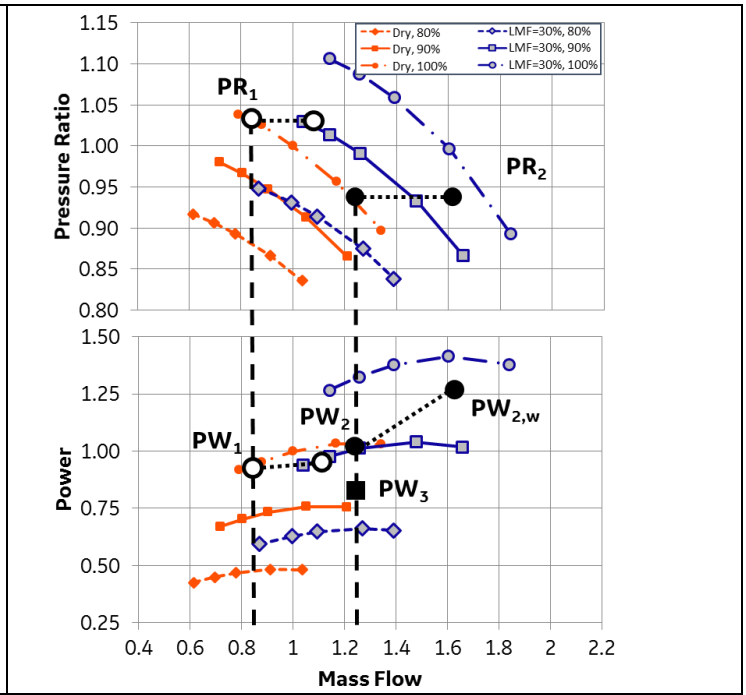

Figure 8: Compressor map (80%-90%-100%) in dry and wet conditions (LMF = 30%) for design inlet pressure p_1/p_n=1. Two different operating points, part-flow and overflow are depicted by plain dots and filled dots, respectively. An operating point at same total mass flow is marked with a filled square

Considering the overflow conditions, for a given normalized flow coefficient (i.e. ϕ = 1.2), the pressure ratio PR_2 is achieved in dry

conditions at the rated speed (100%) and at a speed between 90% and 100% in wet conditions. Due to the combination of the shift-tilt effect on the PR curve and the presence of an intersection point with the dry curves (Figure 6, central panel), at the overflow the compressor delivers the same (or lower) PR for a given speed. As a result, the speed reduction is not enough to avoid increments of the overall gas power that moves from PW_2 to an higher value $PW_{2,w}$.
In summary, for a fixed PR, the wet operation of a CC yields substantially to the same performance from design conditions to part-flow, while increments of power are obtained moving towards overflow. It should be noted that the result considers the worst condition (LMF = 30%) with p_1/p_n=1; either increasing the suction pressure or decreasing the LMF yields to reduced regions of power increments.
The same analyses can be performed considering the inlet total mass flow. In Figure 8 the same operating points discussed in Figure 7 have been depicted in terms of mass flow: the increased mass flow yields to higher compression power that is compensated by the shift and tilt of the PR curves. It is worth to notice that for a given mass flow, namely a situation in which the liquid injection is compensated by a consistent gas mass flow reduction, the absorbed compression power reduces for a given delivered PR: thanks to the shift of performance characteristics, the same service can be delivered at a lower speed and thus lower power (points PW_3, PR_2 in Figure 8).

Compressor surge limit in wet conditions

A surge test has been performed to assess the operability toward surge and define the surge control line. Starting form a stable part-flow condition, the inlet flow coefficient has been reduced until the surge limit criterions were met. The limit criterion being, or head rise to surge getting flat or very low frequency sub-synchronous vibration showing up. To keep the desired LMF, both gas mass flow and injected liquid mass flow have been thoroughly controlled during the test. Figure 9 shows the transient behavior of the peak-to-peak radial vibrations in comparison with the normalized pressure ratio. In the near-surge region, the liquid has the effect to increase the overall direct vibrations (roughly from 2μm to 4μm) and the vibration behavior is like what showed in Figure 15 relevant to the slug test. Two different behaviors can be highlighted: up to 5% LMF, the surge region is reached after a consistent flattening of the PR (Figure 9, center and bottom). In this condition, the compressor and the rig are not showing the triggering of inception of dynamic activity. For larger LMF (only LMF 30% is shown), the PR increases continuously. Despite the PR has an increasing trend, local fluctuations of PR and flow coefficient are observed, thus the machine operation is not namely stable.
In Figure 10 (top) the reduction of surge line flow coefficient ($\phi_{surge,wet}/\phi_{surge,dry}$ -1) is reported. The liquid is responsible for roughly 5% - 7% of surge limit reduction, however it is worth noting that the increased pressure ratio of the surge point yields a direct comparison with a higher speed dry curve against which the operating range is slightly increased Figure 10 (bottom).

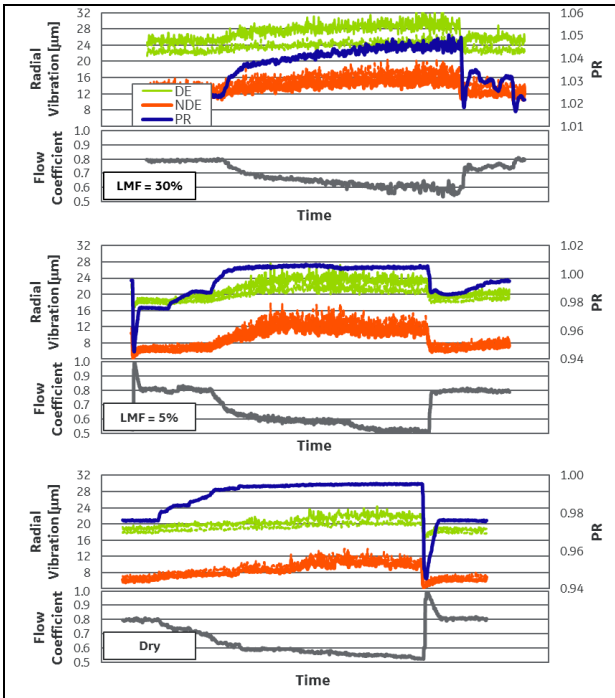

Figure 9: Surge test: time evolution of DE and NDE radial vibrations, normalized PR and normalized flow coefficient. LMF = 30% (top), LMF = 5% (center), dry (bottom) for design speed and p_1/p_n=1.

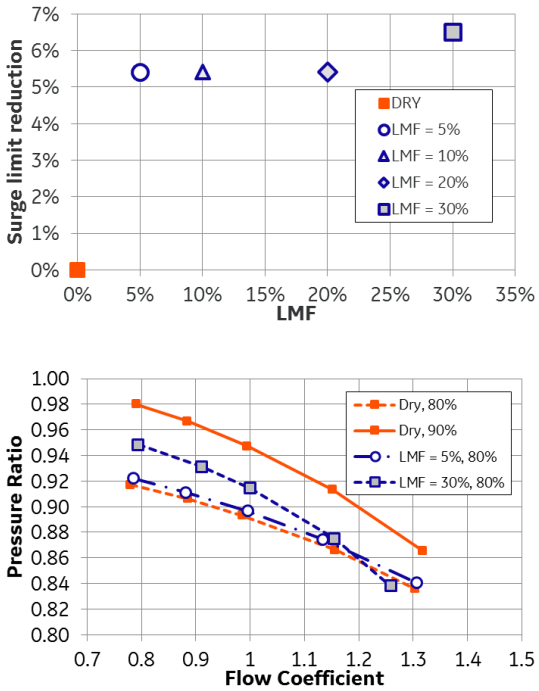

Figure 10: Surge limit flow normalize flow coefficient reduction against dry surge line (top). Normalized pressure ratio at 90% speed (LMF= 5%-30%) compared with dry curve at same speed (90%)

Compressor fouling and washing
Compressor runs about 1400h in dry conditions before starting the running in wet conditions. After this 1400hrs, it was observed a decay of performance with respect to the Factory Acceptance Test FAT (ASME-PTC10 Type2 test). A 72h continuous wet run, injecting water (LMF=30%) at the MCS, allowed a complete recovery of the Type2 performance. The effect is most likely due to the deep washing produced by the mechanical action of the liquid droplets impacting on the compressor surfaces). In Figure 11 the performances (normalized polytropic efficiency) are shown.

Starting from the clean condition reached during the washing, a fouling test was performed. Limited amount of liquid was injected keeping the suction temperature at a value high enough to allow the liquid vaporization along the flow path. Liquid vaporization resulted in a solid particles deposition on the compressor surfaces that, ultimately, accumulated generating the compressor fouling. After the fouling test a significant decay of the performance was observed: compressor efficiency reached values below those observed after the whole wet campaign.

Following the completion of the fouling test, a light washing cycle was performed and the dry performance of the compressor were measured again showing a consistent recovery of the efficiency.

From this test it seems possible that either very low LMFs (LMF < 1%) and high temperatures and dry saturated operation of heavy rich gas are likely to trigger significant fouling and compressor performance degradation. However, the washing cycles are an effective measure to recovering performance. Depending on the duration of the cycle a partial or complete recovery can be reached. It seems also clear the washing cycles effectiveness depends on the mechanical action of the liquid on the surface, thus proper wet tolerant material selections should be devised if frequent washing cycles are planned through the compressor lifecycle, moreover the frequency and execution of the washing cycles should be defined upon the compressor operation plan under OEM advisory.

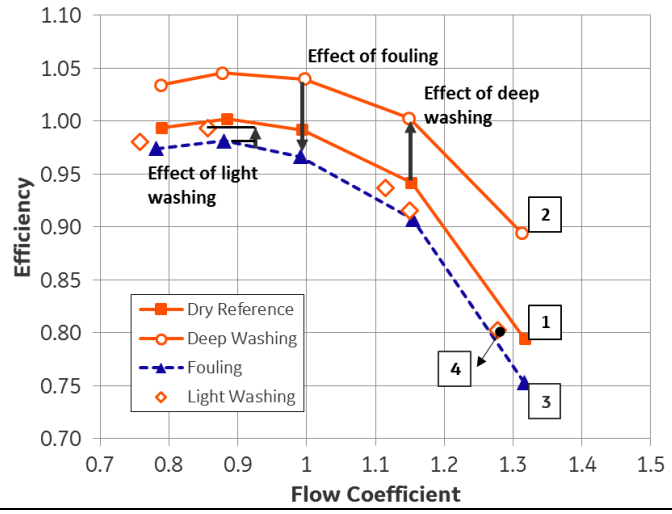

Figure 11: Fouling and washing effects on compressor efficiency in dry conditions. Deep washing curve (curve 2): deep washing cycles from Dry reference (curve 1). Fouling (curve 3): compressor fouling from deep washing curve. Light washing (points 4): light washing cycle from compressor fouling (only some points have been taken).

MECHANICAL PERFORMANCE (ROTORDYNAMICS, EROSION)

Axial Thrust Load
API617 does not provide any acceptance criteria in terms of thrust load, there is only a requirement in terms of thrust load design to be taken in account. Maximum design load to be considered is 50% of bearing capability. Thrust load has been measured during the test, both in dry and wet conditions. In all operating conditions thrust load is well within thrust bearing capability, being always well below 20% of thrust capability. The trend of the thrust variation in the operating envelop has been observed as function of rpm, suction pressure and LMF. In the following figures are showed measured data from load cells at fixed speed and suction pressure at different LMF expressed as thrust capability percentage versus compressor flow coefficient (see Figure 12).
Special design of impeller foot seal diameter has demonstrated to mitigate the effect of large LMF variation on axial thrust load.

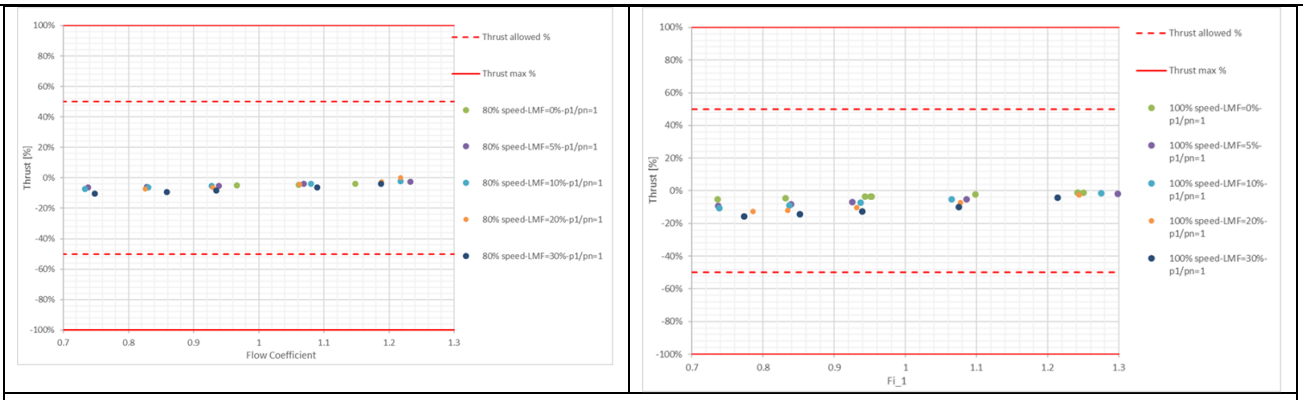

Figure 12: Thrust load measured: lower speed (80%) and p_1/p_n = 1 (left); reference speed (100%) and p_1/p_n = 1 (right).

Erosion test

The erosion meant as loss of material, due to the liquid presence is known to be dependent on the characteristic of the flow and of course of the material erosion resistance. A specific accelerated erosion test has been performed to test the CC internals under continuous severe conditions (low pressure, LMF=20% injecting water to increase the DR). Although the running conditions were very aggressive in terms of potential erosion, the number of running hours in such conditions were limited and the test was performed mainly to demonstrate that no material loss occurred.

Rotordynamic Test

From rotordynamic viewpoint the major tests are listed here below:

- Stability evaluation in wet gas operation
- Slug test
- Wet startup

Stability evaluation in wet gas operation

Stability evaluation was performed using Operational Modal Analysis (OMA) according to the OEM best practice already presented in previous works, see Baldassarre. The main OMA assumption is to consider steady state process condition. For this reason, vibration data from performance tests were analyzed. The baseline was indeed showing very high stability with Log Dec values above 1 (as a reference 0.1 is the minimum acceptable level according to API 617). This behavior is attributed to the presence of a PDS on balance piston as anticipated in the rotordynamic design paragraph. Figure 13 is relevant to p_1/p_n=1 suction pressure and 100% running speed.

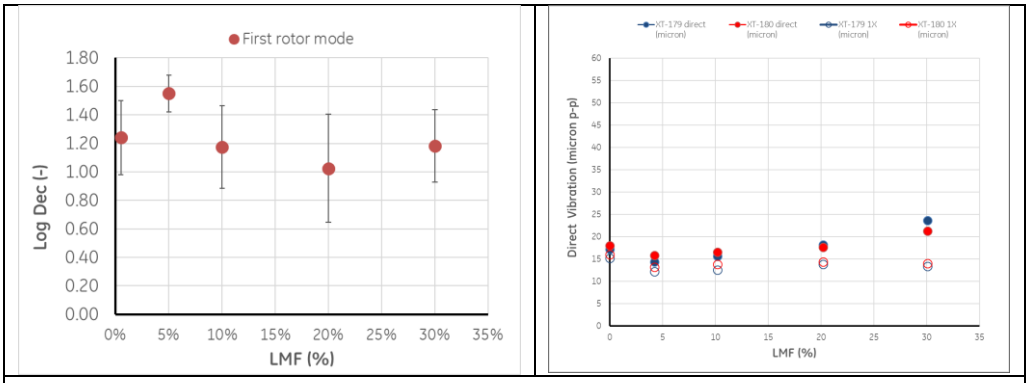

Figure 13: Log Dec vs. LMF (left), vibration amplitude vs. LMF (right).

Figure 13 left shows the trend of the Log Dec versus LMF. Two different compressor operating conditions are shown (high and low flow according to the compressor curve right and left limits). There is not a clear trend here and the experimental uncertainty sometimes makes the numbers very similar between the two test conditions. The major outcome was no detrimental effect comes from the liquid since the stability of the first mode is always at very comfortable levels. These results extend the validity of the experimental campaign already performed by the OEM on the WGC prototype, see Vannini, Bertoneri. The experimental identification uncertainty which is plotted through the error bars in the same Figure 13, was quantified both using a different cut-off frequency for the examined vibration signals and different identification algorithms. Analysis was performed using a commercial tool, see Artemis.

Figure 13 right shows the vibration amplitude trend versus LMF. It is evident the presence of the liquid was increasing the direct vibration level, but this was always within typical values for dry operating conditions (e.g. 25microns) and well below alarm level. At the same time from this plot is possible to see which the main source for this increase was: the 1Xrev component was overall constant so the liquid was not increasing the unbalance-like excitation, but it was acting on other frequency components. To better understand this point, the waterfall plot for one out of four lateral vibration probes during a transitional phase where LMF injection is changed in the range from 0% to 30% is presented in Figure 14. The vibration axis scale was very much enlarged to better highlight the sub synchronous activity which was within 1micron level per each discrete frequency. It is clear enough when the liquid was present there was a sort of widespread noise and some regions were more active than others (e.g. the first natural frequency region around 120-130Hz). On the contrary when the liquid injection was stopped the spectrum was much cleaner. This experimental evidence was matching with the results from the previous WGC prototype.

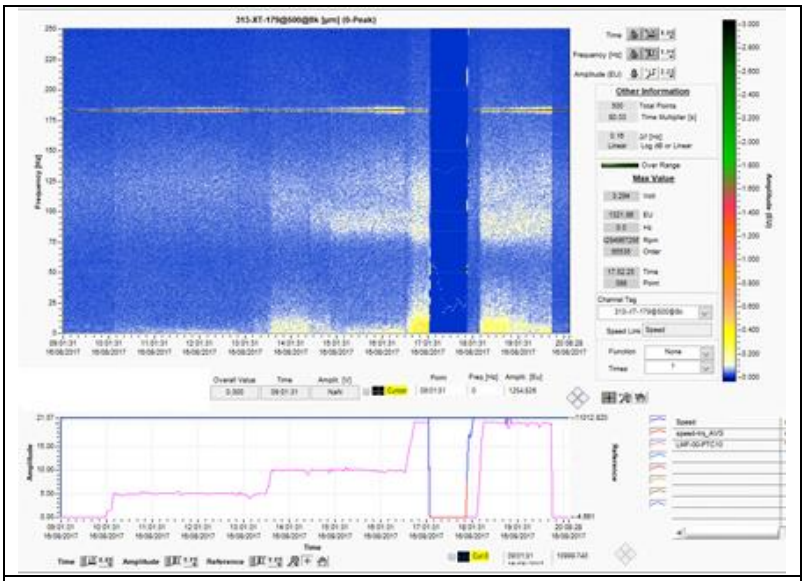

Figure 14: Lateral vibration waterfall plot and relevant LMF trend

Slug test

This test was performed with compressor running at constant suction pressure and speed. Suddenly the liquid was injected into the suction pipe until reaching a desired LMF target and then stopped. The same sequence was then repeated at a higher LMF level. Typically, three LMF steps were tested (0-10%, 0-20% and 0,30%). The compressor vibrations were monitored during these transients through the following plots (Figure 15).

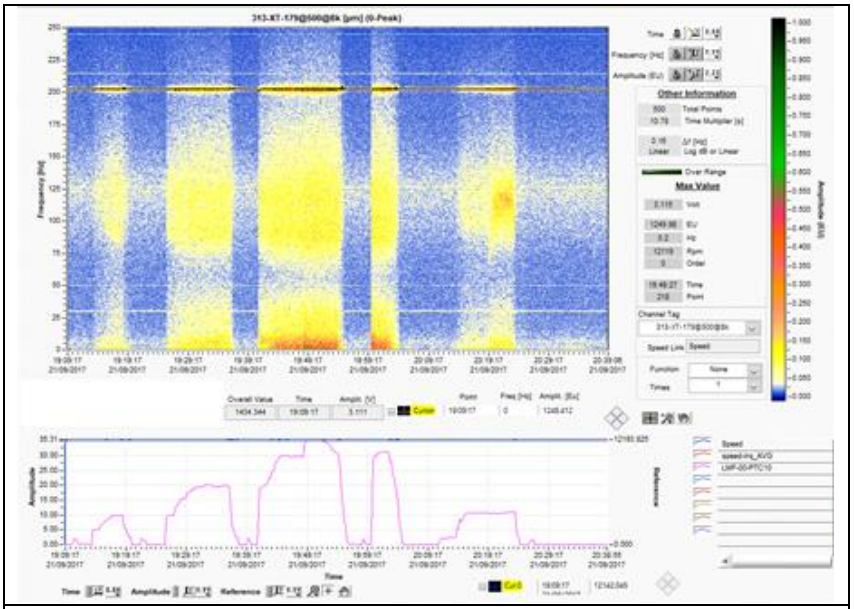

Figure 15: Waterfall plots during slug testing.

The maximum vibration level was still within reasonable values (around 30microns) even if no specific acceptance criteria exist for

this test. The vibration spectrum was still showing the "background noise" feature with an additional indication: the higher the LMF the wider is the region affected by this noise. These results are overall in line with those from Vannini, Bertoneri.

Wet startup from flooded condition

When machine was stopped and depressurized, the flow path region was filled with liquid up to the shaft end seals. Then machine was pressurized with process gas and restarted. It was interesting to compare a dry startup versus a wet one, see Figure 16. No major difference was visible.

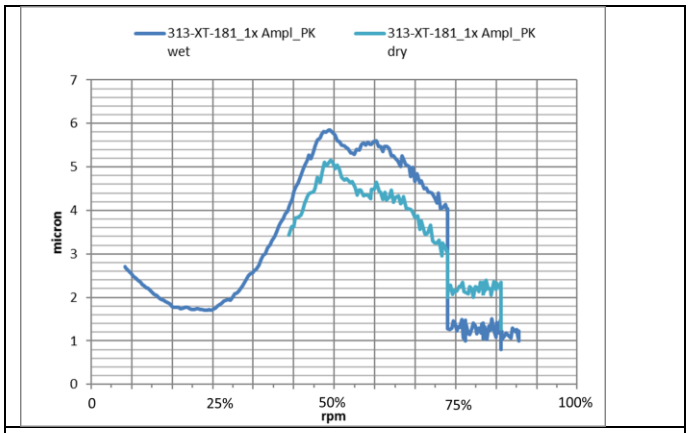

Figure 16: Vibration levels measured in dry vs. wet startup

Overall, the compressor rotordynamic behavior was satisfactory being the vibration level comparable to the one during dry operations and the stability was always verified.

BUNDLE INSPECTION

A complete bundle inspection was carried out at the end of the test campaign to verify the status of the WGC internals. Borescope inspections were also carried out during several stages of the compressor operation, including pre, during and post-test campaign. The main intention was to closely monitor fouling development and material deposition build up on the WGC internals, as well as to detect any potential macroscopic signs of damage to the components. In addition, since the WGC accumulated dry run operation for about 1400hrs before wet run campaign and 400hrs afterward, the purpose was also to establish a baseline and separate the effects of both dry and wet operation over the compressor internals. Due to the presence of special instrumentation installed on the machine, only suction volute and discharge scroll could be inspected; dimensional constraints of the sensing element prevented also the access to small clearances such the ones of the impeller seals to verify any signs of potential wear. Although qualitative (visual inspection), the borescope inspection provided useful indications showing fouling build up trend within the wet test campaign.

The inspection of the compressor has been accomplished through disassembly, visual inspection, cleaning, dimensional and geometric checks. Visually inspection consists in checking about macroscopic defects (scorings, erosion-corrosion, porosity, FOD, linear indications, scratches, missing material, nicks and rubbings, coating detachment). As a marginal note it should be noticed that the WGC bundle inspection was postponed after roughly 1.5 months after the WGC test completion (during that time the compressor has been mainly shut down and accumulated only 400hrs of run in dry conditions with rich gas); however, given the previous experience, the additional run is expected to have negligible effects.

The WGC bundle was then removed from the casing for thorough examination:

- Visual inspection showed solid fouling deposition over the entire flow path. This was expected considering that fouling test was carried out at the end of the test campaign. Deposit thicknesses exceeded 1mm on the discharge area, moreover the deposits layers were not uniform on all surfaces, indicating possibility for debris to detach during operation. However, the possible detachments of chunks of solid material has not produced any compatible damage on the internals, thus it is considered not dangerous for the operation. Same type of fouling was also found in the shunt holes feeding the balance piston seal, which were consequently found plugged in about 50% of the cases. Therefore, special attention shall be put on dimensioning of the extraction holes. The washing of the compressor has demonstrated to be a powerful way to remove fouling and overcome the plugging of the holes
- PDS pockets and swirl brakes vanes still free and open
- The abradable surfaces facing impeller seals and shaft end labyrinth seals were found with one isolated deep sign of worn through the whole circumference. The cause seems most likely associated to some hard debris temporary entrapped in the clearances
- Both DGS cartridges were found functional but contaminated by presence of wax. Wax deposits were also found in some of the drains. It is worth to note that those drains were never operated during the test (including also the DGS seal gas supply ones where no deposits were expected to be found). Following DGS cartridges examination confirmed a substantial presence of wax which fully impinged the lower sector (Figure 17) and light running marks on seat and seal face. Despite that both seals were still

in a condition to accomplish their task. Wax accumulation can be reduced through a dedicated drain strategy to be set case by case depending mainly on the gas composition.

Figure 17: DE and NDE seals inspection: barrier seal stationary part DE and sleeve for barrier seal (top left), DE seal and NDE seal (top right), stationary seal face (bottom left), rotating seal (bottom right)

- Journal and thrust bearings were inspected and no signs of abnormal wearing was noted, indicating correct functioning of the bearing.
- All bundle components were cleaned to allow for visual inspection of the base material underneath. Coatings on suction plenum and IGV diaphragm were found in good conditions with no signs of scratches or coating detachment. No signs of erosion nor cracks or linear indications were noticed. It is worth to highlight the fact that on dry compressor applications protective coatings or material intrinsically resistant to pitting are applied normally on suction and first stage only; inspection of the WGC prototype compressor has showed, through the comparison between coated and not coated stator parts, the need of application of protective coatings on all stator parts since pitting has been found on not coated stator parts.

FURTHER WORKS

This experience highlighted operational modes that are typical of a liquid tolerant compressor and provided a full understanding on machine behavior. Detailed discussion of other topics that are not included in the present article, like wet performance predictability, seal gas treatment and overall fouling phenomenology may be a subject of further works.

CONCLUSIONS

All over the test period, 850hrs in wet condition, the compressor behavior was satisfactory both in steady and transient operations, highlighting operational modes that are typical of the liquid tolerant compression. The compressor performance is affected by the presence of liquid, as expected. PR slope is increased and rotated around a point which depends on the suction pressure; this means that PR may increase or decrease depending on the operating point and the suction pressure with respect to dry operation. Absorbed power is increasing mainly due to the larger mass flow. Surge line is weakly affected by the wet conditions; therefore, operating range is in line or slightly increased compared to dry conditions.

Thanks to the specific rotordynamic design the radial vibrations and thrust are within the API 617 specifications under the liquid range considered.

Bundle inspection has shown significant presence of solid deposits (fouling), nevertheless compressor is still able to accomplish its function. Performance degradation, due to fouling accumulation, can be controlled through periodic online washing cycles to be set case by case. Coatings on compressor suction were found in good condition after the test with no damages or detachments. No mechanical damages due to erosion has been observed. This is in line with OEM expectation given the qualification carried out in lab

on material and coating. Presence of pitting was found on not coated stator components; therefore, in wet gas application it is needed the application of protective coating on all wetted surfaces.

The test campaign performed, and its results are encouraging for the application of WGC technology on field. Then, the next step is to apply this technology where the advantage of simplifying separation units or taking care of scrubber carryover are relevant. In the near term, applications where the compressor life span or the scheduled maintenance period allows for frequent inspection (borescope) are the most suitable for the adoption of this technology. This will provide a further step in the technology readiness level.

NOMENCLATURE

BN = Bentley Nevada
CC = Centrifugal Compressor
DE = Drive End
DGS = Dry Gas Seal
DR = Density Ratio
EOS = Equation of State
IGV = Inlet Guide Vane
LDE = Liquid Droplet Erosion
LMF = Liquid Mass Fraction
LT = Level Transmitter
NDE = Non-Drive End
OEM = Original Equipment Manufacturer
PDS = Pocket Damper Seal
PR = Pressure Ratio
PT = Pressure transducer
RTD = Resistance Temperature Detector
SGCS = Seal Gas Conditioning Skid
SGP = Seal Gas Panel
SSV = Sub Synchronous Vibration
TOR = Tooth On Rotor
VFD = Variable Speed Drive
WGC = Wet Gas Compression

FIGURES

REFERENCES

Brenne, L., Bjørge, T., Bakken, L. E., Hundseid, Ø., "Prospect for Sub Sea Wet Gas Compression", ASME Turbo Expo 2008, GT2008-51158

Brenne, L., Bjørge, T., Gilarranz, J. L., Koch, J. M., Miller, H., "Performance Evaluation of a Centrifugal Compressor Operating Under Wet Gas Conditions", Turbomachinery Symposium 2005

Bertoneri, M., Duni, S., Ransom, D., Podestà, L., Camatti, M., Bigi, M., Wilcox, M., "Measured Performance of Two-Stage Centrifugal Compressor under Wet Gas Conditions", ASME Turbo Expo 2012, GT2012-69819

Fabbrizzi, M., Cerretelli, C., Del Medico, F., D'Orazio, M., "An Experimental Investigation of a Single Stage Wet Gas Centrifugal Compressor", ASME Turbo Expo 2009, GT2009-59548

Grüner, T. G., Bakken, L. E., "Instability Characteristic of a Single-stage Centrifugal Compressor Exposed to Dry and Wet Gas", ASME Turbo Expo 2012, GT2012-69473

Minghong, L., Qun, Z., "Wet Compression System Stability Analysis Part I", ASME Turbo Expo 2004, GT2004-54018

API 617, Axial and Centrifugal Compressors and Expander-Compressors for Petroleum, Chemical and Gas Industry Services, Eight Edition, September 2014, American Petroleum Institute, Washington, D.C.

Artemis, Software for Modal Analysis, Structural Vibration Soutions, http://www.svibs.com/.

Baldassarre L., Guglielmo A., Catanzaro M., de Oilveira Zague L., Timbo Silva L., Ishimoto L., Accorsi Miranda M., Operational Modal Analysis Application For The Measure Of Logarithmic Decrement In Centrifugal Compressor, Proceedings of the 44th Turbomachinery Symposium, 2015, Houston.

Bertoneri M., Vannini G., "US 2017/0211595, Extracting dry gas from a wet-gas compressor", July 27, 2017.

Li J., San Andres L., Vance J., "A bulk flow analysis of multiple pocket gas damper seals", Journal of engineering for gas Turbines and Power, Vol. 121 April 1999.

Vannini G., Bertoneri M., Del Vescovo G., Wilcox M., "Centrifugal Compressor Rotordynamics in Wet Gas Conditions", Proceedings of 43rd Turbomachinery Symposium, Houston, USA, 2014.

Vannini G., Cioncolini S., Del Vescovo G., Rovini M., "Labyrinth Seal and Pocket Damper Seal High Pressure Rotordynamic Test Data", Journal of Engineering for Gas Turbines and Power, February 2014, Vol. 136.

Vannini G., Bertoneri M., Nielsen K. K., Iudiciani P., Stronach R., "Experimental Results and Computational Fluid Dynamics Simulations of Labyrinth and Pocket Damper Seals for Wet Gas Compression", Journal of Engineering for Gas Turbines and Power, May 2016, Vol. 138.

Falomi S., Scarbolo L., Bertoneri M., Ferrara V., Performance test of a wet tolerant impeller and validation of wet compression predictive model, Proceedings of the 45th Turbomachinery Symposium, 2016, Houston.

ACKNOWLEDGEMENTS

The authors gratefully acknowledge Equinor and Chevron for their active participation in the joint Industrial Program (JIP) which includes the test campaign reported in the present paper. The authors gratefully acknowledge Equinor and the K-Lab department for their cooperation in the test commissioning and execution.